

# Quantitative MRI of kidneys in renal disease

Timothy L. Kline<sup>1</sup>, Marie E. Edwards,<sup>2</sup> Ishan Garg,<sup>1</sup> Maria V. Irazabal,<sup>2</sup>  
Panagiotis Korfiatis,<sup>1</sup> Peter C. Harris,<sup>2</sup> Bernard F. King,<sup>1</sup> Vicente E. Torres,<sup>2</sup>  
Sudhakar K. Venkatesh,<sup>1</sup> Bradley J. Erickson<sup>1</sup>

<sup>1</sup>Department of Radiology, Mayo Clinic College of Medicine, 200 First St SW, Rochester 55905, MN, USA

<sup>2</sup>Division of Nephrology and Hypertension, Mayo Clinic College of Medicine, Rochester, MN, USA

## Abstract

**Purpose:** To evaluate the reproducibility and utility of quantitative magnetic resonance imaging (MRI) sequences for the assessment of kidneys in young adults with normal renal function (eGFR ranged from 90 to 130 mL/min/1.73 m<sup>2</sup>) and patients with early renal disease (autosomal dominant polycystic kidney disease).

**Materials and methods:** This prospective case–control study was performed on ten normal young adults (18–30 years old) and ten age- and sex-matched patients with early renal parenchymal disease (autosomal dominant polycystic kidney disease). All subjects underwent a comprehensive kidney MRI protocol, including qualitative imaging: T1w, T2w, FIESTA, and quantitative imaging: 2D cine phase contrast of the renal arteries, and parenchymal diffusion weighted imaging (DWI), magnetization transfer imaging (MTI), blood oxygen level dependent (BOLD) imaging, and magnetic resonance elastography (MRE). The normal controls were imaged on two separate occasions  $\geq 24$  h apart (range 24–210 h) to assess reproducibility of the measurements.

**Results:** Quantitative MR imaging sequences were found to be reproducible. The mean  $\pm$  SD absolute percent difference between quantitative parameters measured  $\geq 24$  h apart were: MTI-derived ratio =  $4.5 \pm 3.6\%$ , DWI-derived apparent diffusion coefficient (ADC) =  $6.5 \pm 3.4\%$ , BOLD-derived  $R2^*$  =  $7.4 \pm 5.9\%$ , and MRE-derived tissue stiffness =  $7.6 \pm 3.3\%$ . Compared with controls, the ADPKD patient's non-cystic renal parenchyma (NCRP) had statistically significant differences with regard to quantitative parenchymal measures: lower MTI percent ratios ( $16.3 \pm 4.4$  vs.  $23.8 \pm 1.2$ ,  $p < 0.05$ ), higher ADCs ( $2.46 \pm 0.20$  vs.  $2.18 \pm 0.10 \times 10^{-3}$  mm<sup>2</sup>/s,  $p < 0.05$ ), lower  $R2^*$ s ( $14.9 \pm 1.7$  vs.  $18.1 \pm 1.6$  s<sup>-1</sup>,  $p < 0.05$ ), and lower

tissue stiffness ( $3.2 \pm 0.3$  vs.  $3.8 \pm 0.5$  kPa,  $p < 0.05$ ).

**Conclusion:** Excellent reproducibility of the quantitative measurements was obtained in all cases. Significantly different quantitative MR parenchymal measurement parameters between ADPKD patients and normal controls were obtained by MT, DWI, BOLD, and MRE indicating the potential for detecting and following renal disease at an earlier stage than the conventional qualitative imaging techniques.

**Key words:** Autosomal dominant polycystic kidney disease—Magnetic resonance imaging—Quantitative magnetic resonance imaging—Segmentation—Total kidney volume

Renal parenchymal disease and dysfunction is a major cause of morbidity, as well as health care costs in the U.S. In 2014, there were 4.5 million American adults diagnosed with kidney disease [1]. Kidney disease also ranks in the top ten causes of death [2]. Unfortunately, there are limited tests available today to evaluate renal function and/or disease progression. Glomerular filtration rate (GFR) is generally considered the best indicator of renal function [3]. The most commonly used measurement technique to estimate GFR (eGFR) utilizes serum creatinine levels as a surrogate measure of kidney function [4]. However, these measurements can vary widely and patients with serum creatinine levels within the “normal range” may actually have significant reduction in renal function [5]. Therefore, quantitative techniques that can add to the assessment of renal structure and function are drastically needed.

Quantitative MRI techniques provide new imaging biomarkers that could facilitate a comprehensive characterization of the kidney tissue and function in various states of health and disease [6]. These quantitative MR techniques could aid in a deeper understanding of the

function and composition of a patient's renal tissue which could provide a more accurate and earlier assessment of renal disease and facilitate earlier interventions to halt or slow down renal disease progression [7–23].

In an attempt to evaluate these newer quantitative MR techniques, we developed an extensive MR imaging protocol that explores a number of newly established quantitative MRI techniques in order to test the reproducibility of the approaches, as well as explore their utility in the evaluation of young patients with autosomal dominant polycystic kidney disease (ADPKD). In particular, to assess whether differences in non-cystic renal parenchyma (NCRP) was quantifiable and different than in age matched controls, we designed a pilot study evaluating ten young (aged 18–30) ADPKD patients with normal renal function, and ten age- and sex-matched normal controls.

## Materials and methods

### Cohort

Approval from our Institutional Review Board was obtained for this study which adheres to the Declaration of Helsinki. This clinical trial was registered in 2014 (Registration# 000000000). A statement of informed consent was obtained from all study participants. Ten ADPKD patients (6F, 4M) between the ages of 18–30 and ten age- and sex-matched normal non-ADPKD controls were enrolled in this study. A careful set of criteria were used for determining inclusion/exclusion of participants (Table 1).

Once the study subject gave informed consent, they were asked to complete a health questionnaire and their height and weight were measured. The MRI was performed between 6 and 7 am on all subjects to minimize potential diurnal variations in renal physiologic function.

Subjects fasted the previous evening from 8 pm to enable a controlled hydration status for all subjects. Each normal subject was also studied a second time using the same imaging parameters within 1–7 days of the original MR to determine day-to-day inherent subject variability. Urine and blood samples were also collected on the day of the examination. Standard blood pressure measurements were made on all patients in the MR scanning room prior to all MR studies. MR scan for all study participants was completed between 12/18/2014 and 03/24/2016.

### MRI data

All MR acquisitions were acquired on a GE 3T scanner (GE Medical Systems, Discovery MR750w) in the supine position utilizing a multichannel surface coil. No intravenous contrast was used. The sequences included in the imaging protocol were conventional SSFSE axial, coronal, and sagittal scout images followed by T1 (coronal lava sequence, with 10° flip angle, and reconstructed voxel resolution in plane of ~1 mm, and slice thickness of 3 mm) and T2-weighted (coronal fast spin echo, TE = 100 ms, TR = min, with reconstructed voxel resolution in plane of ~1 mm, and slice thickness of 3 mm) breath hold images for anatomic details.

Following scout and routine anatomic pulse sequences and quantitative pulse sequences were obtained. Axial, breath-held diffusion weighted sequences were acquired with spin echo pulse sequence and *b*-values of 0, 20, 30, 40, 60, 80, 100, 120, 140, 160, 180, 200, 240, 300, 400, 500, 600, 700, 800, 900, and 1000 s/mm<sup>2</sup>. Blood oxygen level-dependent (BOLD) images of the kidneys were acquired with a fast gradient echo pulse sequence (TR = 90 ms, flip angle = 20°) utilizing 12 different consecutive echo times of 3, 8, 13, 18, 22, 27, 32, 37, 42,

**Table 1.** Selection criteria used in this study to select ADPKD patients and controls

Inclusion	Exclusion
Male/female between 18 and 30 years of age, inclusive Must have a glomerular filtration rate (GFR) of ≥60 mL/min (CKD-EPI equation)	Clinically significant concomitant systemic disease that in the investigator's opinion may place the subject at risk or are known to affect the kidney. This includes, but is not limited to, concurrent or history of lupus, hepatitis B or C, amyloidosis, etc.
Ability to provide written informed consent prior to initiation of any study-related procedures, and ability, in the opinion of the principle investigator, to comply with all requirements of the study	Subjects with diabetes mellitus (fasting glucose > 126 mg/dL or on treatment with insulin or oral hypoglycemics)
<i>ADPKD patient group only</i> diagnosis of ADPKD [diagnosis for this population is based on Ravine et al. and requires several cysts in each kidney (3 if by sonography, 5 if by computed topography (CT) or MRI in those with a family history of ADPKD and 10 cysts (by radiologic method) in each kidney and exclusion of other cystic kidney diseases if there is no family history]	Urinary protein excretion Abnormal urinalysis suggestive of concomitant glomerular disease Subjects having contraindications to or interference with MRI assessments. [e.g., ferromagnetic metal prostheses, aneurysm clips, severe claustrophobia, large abdominal/back tattoos] Subjects with supine blood pressure, after resting for ≥3 min, > 140/90 mmHg or are taking blood pressure medications Female subjects that are pregnant <i>Control group only:</i> previous personal or family history of kidney disease

47, 52, and 56 ms. MT images were acquired with and without an offset frequency pulse of 1.5 kHz using a spoiled gradient (SPGR) sequence with TE = 80 ms, TE = 3.2 ms (with in-plane voxel resolution of ~1.0 mm, and slice thickness of 8.0 mm).

Following breath-held coronal and oblique coronal fast imaging employing steady-state acquisition (FIESTA) localizing images of the renal arteries, cine phase contrast renal blood flow acquisitions were obtained perpendicular to each renal artery utilizing a velocity encoding (VENC) value of 100 cm/s. Finally, MR Elastography acquisitions were obtained utilizing a passive driver for each kidney positioned posteriorly over each kidney. The drivers were placed above the iliac crest and below the 12th rib on either side of the spine. The MR Elastography was a coronal flow compensated, single shot, spin echo, echoplanar sequence performed at 90 Hz frequency. The slices covered the entire anterior to posterior extent of the kidneys with slice thickness of 3 mm.

### *Kidney segmentation*

A trained medical image analyst (Y, >3 years' experience) performed kidney segmentation semi-automatically utilizing the MIROS software package [24]. The software package has an interactive viewer that allows visualization of the image data in coronal, sagittal, and axial planes. Segmentations can be overlaid and edited with a range of interactive tools. The MIROS algorithm was implemented in the Python programming language and has a push-button that starts the interactive tool for defining crude polygon contours of the kidneys. We performed the MIROS method on the T2-weighted images, obtaining user input every third slice (every 9 mm). After segmentation of each kidney by MIROS, the interactive tools were used to perform quality assurance and finalize the segmentation. Total kidney volume was measured from these segmentations. Cyst segmentations were performed manually and were used to calculate cystic burden of the kidneys. Cyst segmentations took 45–60 min per case dependent on disease severity. A registration-based approach was used to transfer the kidney and cyst segmentations to the BOLD, DWI, and MT acquisitions in order to measure the quantitative MRI parameters in NCRP regions. MRE data were segmented manually.

### *Image processing*

In house software was developed to process the majority of the quantitative scans. Here, we detail the processing steps carried out for each quantitative scan.

**BOLD** The BOLD protocol obtained a series of images with 12 different echo times. In order to correct for motion, a 2D affine registration was performed which

registered each echo time to the lowest that was performed. Mono-exponential fitting was performed on a pixel-wise bases on the series of images in order to derive  $R2^*$ , which is inversely related to the rate of spin dephasing ( $1/T2^*$ ) and is here used as the BOLD parameter (a surrogate for the amount of deoxyhemoglobin in the blood)

**DWI** The DWI protocol obtained a series of images with different diffusion weightings, 21 in total. In order to correct for motion, a 2D affine registration was performed which registered each b-value to the lowest that was performed. Both mono-exponential and bi-exponential pixel-wise fitting were performed in order to derive apparent diffusion coefficient (ADC) and intravoxel incoherent motion measurements (IVIM). With IVIM, decomposition of the signal into pure diffusion (D), and pseudo-diffusion ( $D^*$ ) (with contributions from perfusion and tubular flow) is achieved. Also perfusion fraction (PF) can be calculated. These are derived from  $S = S_0[PF \cdot e^{-b \cdot D^*} + (1 - PF) \cdot e^{-b \cdot D}]$ , where  $S_0$  is the signal at  $b = 0$ .

**MT** Two image acquisitions were performed, one with, and one without an offset RF pulse at 1.5 kHz. Due to the fact that the two images were acquired over different breathholds, image registration was used to improve alignment of the two scans. The magnetization transfer ratio was then calculated as  $(M_0 - M_S) / M_0 \times 100\%$ .

**MRE** Tissue stiffness was measured on a separate workstation (Advantage Windows, AD 4.0, GE) with anatomical images and corresponding stiffness maps displayed side by side. Region of interest (ROI) was drawn on anatomical images excluding the kidney edges, renal hilum, and pelvis. The ROIs were then copy pasted on to stiffness maps to obtain the measurement of tissue stiffness values (kilopascals, kPa). ROIs were initially drawn by a research trainee (MD) and verified by board-certified abdominal radiologist with 10 years' experience in MR Elastography. The ROIs were copy pasted onto the stiffness maps to obtain stiffness values. The stiffness obtained with each ROI was averaged to the mean stiffness of each kidney. In the case of ADPKD patients with cysts, ROIs excluded all cysts identified on the magnitude (anatomical image) and only NCRP stiffness was measured.

### *Analysis*

The median of the quantitative values within the NCRP was computed in all cases. Correlation coefficients were generated between all imaging biomarkers evaluated in this study. Wilcoxon rank-sum test was used to compare the quantitative parameters in ADPKD patients and

controls, and Bland–Altman analysis [25, 26] was performed to assess test–retest reproducibility of the quantitative techniques.

Renal blood flow (RBF) was measured from the 2D phase contrast images on an AW workstation. A trained radiologist (X) performed the RBF measurements. For each renal artery, measurements were performed three times, and the average value for each artery was used. ROIs were drawn at the border of the renal artery. In the case of multiple renal arteries feeding a single kidney, each artery was measured separately and the sum of the measurements was used as the total RBF perfusing that particular kidney.

### Hemodynamic measurements

Mean arterial pressure was estimated from the measured diastolic blood pressure (DBP) and systolic blood pressure (SBP), where  $MAP \sim DBP + 1/3(SBP - DBP)$  [27]. Renal vascular resistance (RVR) was calculated as  $RVR \sim (MAP/RBF) \cdot 80$  [28]. RBF was first normalized to body surface area (i.e., per  $1.73 \text{ m}^2$ ).

## Results

### Traditional biomarkers

No significant difference between control and patient groups was found for many of the basic biomarkers measured in this study. Table 2 shows results comparing the control vs. ADPKD group. SBP, height adjusted total kidney volume (HtTKV), and cystic index were found to be statistically distinct between the two groups. No statistically significant difference was found for RBF ( $1080 \pm 139$  vs.  $1090 \pm 148$  cc/min).

### Quantitative MR imaging

The extensive quantitative MR imaging protocol was successfully performed in all patients and controls. Examples of traditional T2-weighted MR images of the ADPKD patients and their matched controls are shown in Fig. 1. Fig. 2 shows examples of both conventional MR images (T1 and T2 acquisitions), as well as the quantitative MR image maps generated from MT, DWI, BOLD, and MRE for an ADPKD patient.

### Reproducibility

Quantitative MR imaging sequences were found to be reproducible. The mean  $\pm$  SD absolute percent difference between quantitative parameters measured  $>24$  h apart (range from 24 to 210 h) for the whole kidney were as follows: MTI-derived ratio =  $4.5 \pm 3.6\%$ , DWI-derived apparent diffusion coefficient (ADC) =  $6.5 \pm 3.4\%$ , BOLD-derived  $R2^* = 7.4 \pm 5.9\%$ , and MRE-derived tissue stiffness =  $7.6 \pm 3.3\%$ . Reproducibility of the traditional MR-derived parameters was TKV  $5.1 \pm 3.2\%$  and RBF  $10.1 \pm 7.8\%$ . Fig. 3 shows the Bland–Altman analysis results comparing measurement percent change with the average of the two measurements, as well as the mean and 95% confidence intervals ( $1.96 \times$  SD).

### Correlation

There exist a number of correlations between the biomarkers measured in this study, including quantitative MR measurements, HtTKV, and cystic index. Fig. 4 shows the correlation matrix for all the biomarkers including both control and ADPKD patients.

**Table 2.** Characteristics of the 20 patients in this study comparing the controls to the ADPKD patients for basic parameters

Parameter	Control	PKD	<i>p</i> value
Age (years)	23.0 $\pm$ 3.1	22.5 $\pm$ 3.0	0.521
Weight (kg)	79.0 $\pm$ 12.4	78.0 $\pm$ 23.1	0.791
SBP (mmHg)	111.0 $\pm$ 10.0	125.5 $\pm$ 11.7	0.041
DBP (mmHg)	69.0 $\pm$ 9.7	79.0 $\pm$ 9.0	0.162
Scr (mg/dL)	0.90 $\pm$ 0.14	0.80 $\pm$ 0.17	0.650
uProt (mg/dL)	5.0 $\pm$ 4.4	8.5 $\pm$ 3.8	0.521
MAP (mmHg)	85.8 $\pm$ 8.7	93.7 $\pm$ 9.5	0.057
RVR (mmHg/mL/min/1.73 m <sup>2</sup> )	11.0 $\pm$ 2.2	12.2 $\pm$ 2.1	0.135
CKD-EPI (mL/min/1.73 m <sup>2</sup> )	104.7 $\pm$ 18.3	110.6 $\pm$ 11.7	0.229
HtTKV (mL/min)	178.7 $\pm$ 17.0	346.6 $\pm$ 102.8	<0.001*
Cyst (%)	0.0 $\pm$ 0.0	35.1 $\pm$ 16.3	<0.001*
Total RBF (cc/min)	1083 $\pm$ 157	1045 $\pm$ 139	0.65

Group measurements are shown as mean  $\pm$  SD. Wilcoxon rank-sum test was used to test for statistical significance (*p* value). A *p* value less than 0.05 was considered significant (denoted with asterisk). Here both HtTKV and Cyst (%) were found to be statistically significant between the control vs. ADPKD groups. RBF is measured by 2D-phase contrast MRI. Cyst (%) is the percentage of cysts within the kidneys. *NCRP* non-cystic renal parenchyma, *BOLD* blood oxygen level dependent, *ADC* apparent diffusion coefficient, *DWI* diffusion weighted imaging, *PF* perfusion fraction, *D* true diffusion coefficient, *D\** pseudo-diffusion coefficient, *MTR* magnetization transfer ratio, *MRE* magnetic resonance elastography

Measurement of median MT signal of the whole kidney most closely correlated with HtTKV ( $r = -0.97$ ) as well as cystic index ( $r = -0.89$ ), suggesting that MT imaging can help characterize cystic burden of the kidneys, as shown in Fig. 5. Also shown are the comparisons of cystic burden and HtTKV with the median value

measured within the whole kidneys by BOLD ( $R2^*$ ), and DWI (ADC). Median  $R2^*$  signal of whole kidney correlated with cystic burden ( $r = 0.76$ ) and with HtTKV ( $r = 0.77$ ). Also, the standard deviation DWI signal of parenchyma and whole kidney with cystic burden is 0.72 and 0.74, respectively.



Fig. 1. T2w images of ADPKD patients and their age- and sex-matched controls. A wide range of disease severity was observed in the cohort of young ADPKD patients between the

ages of 18 and 30. Shown in the *bottom left* are age and sex (e.g., 18-year-old male = 18 M), and in *bottom right corner* is height adjusted total kidney volume (HtTKV) in mL/m.

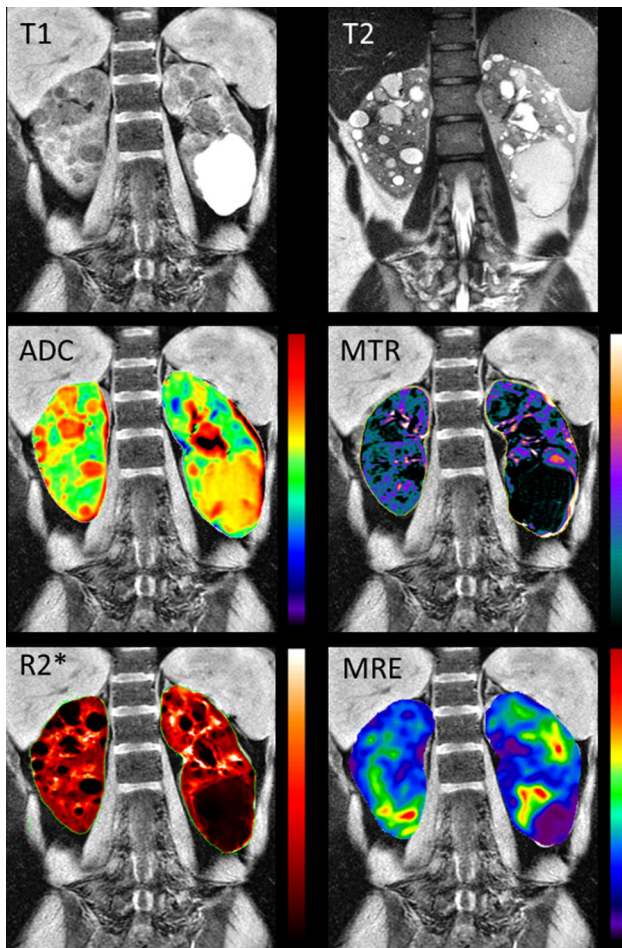


**Fig. 2.** Examples of traditional MR imaging in the *top row*: T1w, T2w, as well as quantitative maps (overlaid on the T1 scan) in the second and third row: apparent diffusion coefficient ‘ADC’ derived from DWI, ‘MTR’ derived from MT, ‘R2\*’ derived from BOLD, and tissue stiffness map derived from MRE for one of the ADPKD patients in this study. The majority of the cysts are simple (*bright* in T2, *dark* in T1). However, one large cyst (bottom of left kidney) is likely proteinaceous. The similar appearance of all cysts in, for example, MTR makes for strong correlation of cystic burden with the derived parameters.

### Quantitative parameters

Many of the quantitative parameters were shown to be significantly different between ADPKD patients and controls, in terms of NCRP measurements. Table 3 highlights these differences in NCRP regions between the control vs. ADPKD group. Compared with controls, the ADPKD patients NCRP had statistically significant differences with regard to having lower MTI percent ratios ( $16.3 \pm 4.4$  vs.  $23.8 \pm 1.2$ ,  $p < 0.05$ ), higher ADCs ( $2.46 \pm 0.20$  vs.  $2.18 \pm 0.10 \times 10^{-3} \text{ mm}^2/\text{s}$ ,  $p < 0.05$ ), higher D ( $2.35 \pm 0.17$  vs.  $2.08 \pm 0.21$ ,  $p < 0.05$ ), lower R2\*s ( $14.9 \pm 1.7$  vs.  $18.1 \pm 1.6 \text{ s}^{-1}$ ,

$p < 0.05$ ), and lower tissue stiffness’s ( $3.2 \pm 0.3$  vs.  $3.8 \pm 0.5 \text{ kPa}$ ,  $p < 0.05$ ). Although it is not statistically significant, ADPKD patients NCRP also had lower perfusion fraction as measured by DWI ( $13.06 \pm 3.8$  vs.  $15.1 \pm 4.0$ ,  $p = 0.2$ ).

### Discussion

This pilot study demonstrates the promise in evaluating quantitative MRI as a potential tool in the early evaluation and intervention in patients with early renal disease. The cohort of young ADPKD patients evaluated in this study is an example of a patient population where more data differentiating fast vs. slow progressors are sorely needed (i.e., young ADPKD patients with normal renal function). The results of this study highlight how quantitative MRI techniques can show differences in structural and functional changes of the kidney associated with ADPKD. These new MR quantitative techniques could be further explored as markers for disease progression in clinical trials evaluating medical treatments attempting to slow, or possibly halt, the disease progression in ADPKD patients at an early age before end stage disease takes hold.

High reproducibility of the quantitative measurements was obtained in the healthy group demonstrating that these techniques are reliable on a routine basis. The reproducibility in all four quantitative MRI protocols was comparable to, and in some cases better than, the traditional MR-derived biomarkers of TKV and RBF. Current techniques for measuring RBF require extensive user interaction—from choosing the imaging plane (double oblique), to manually segmenting the renal arteries and calculating blood flow using the 2D CINE images. We speculate that these considerations, as well as physiological variability, lead to less reproducibility in deriving RBF.

Statistically distinct measurements between ADPKD patients and normal controls were obtained by BOLD, DWI, MT, and MRE. BOLD imaging characterizes tissue oxygenation status, and in this study, we found a reduction in the BOLD parameter (R2\*) which suggests tissue alteration possibly resulting from decreased vascular density and/or changes in tissue viability. Similarly, with DWI we found a reduction in the pseudo-diffusion component (which is a surrogate measure of tissue perfusion) as well as a reduction in the derived perfusion fraction, which, taken together, are compelling evidence for changes in vascular structure and function. The reduction in MTR (measured by MT imaging) likely results from sub-resolution cysts contributing to a reduction in signal (i.e., by partial volume effect) highlighting the possibility that MT imaging could be a better surrogate measure of cystic burden (e.g., compared with segmentation of cysts in T2-weighted MR images). Lastly, MRE found a reduction in tissue stiffness of renal

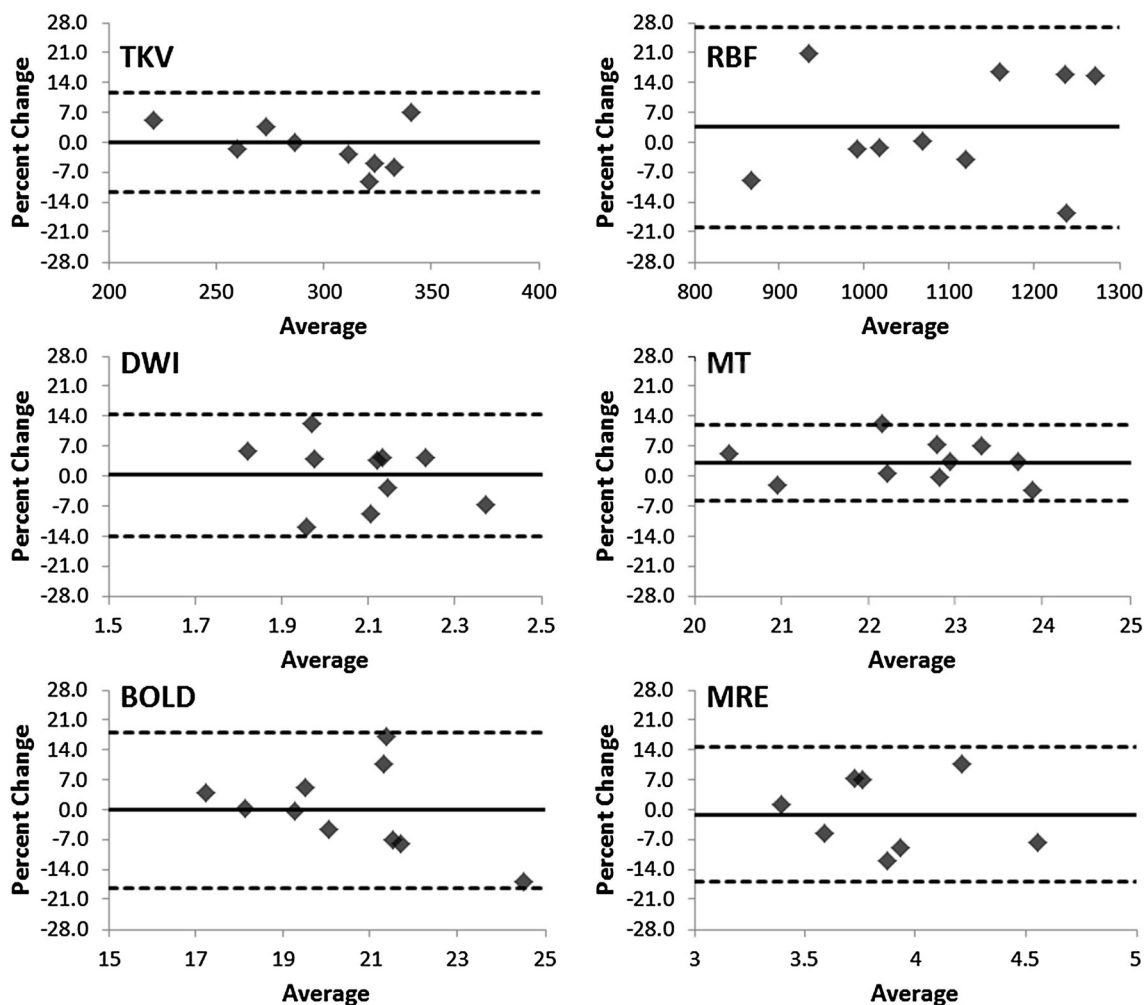


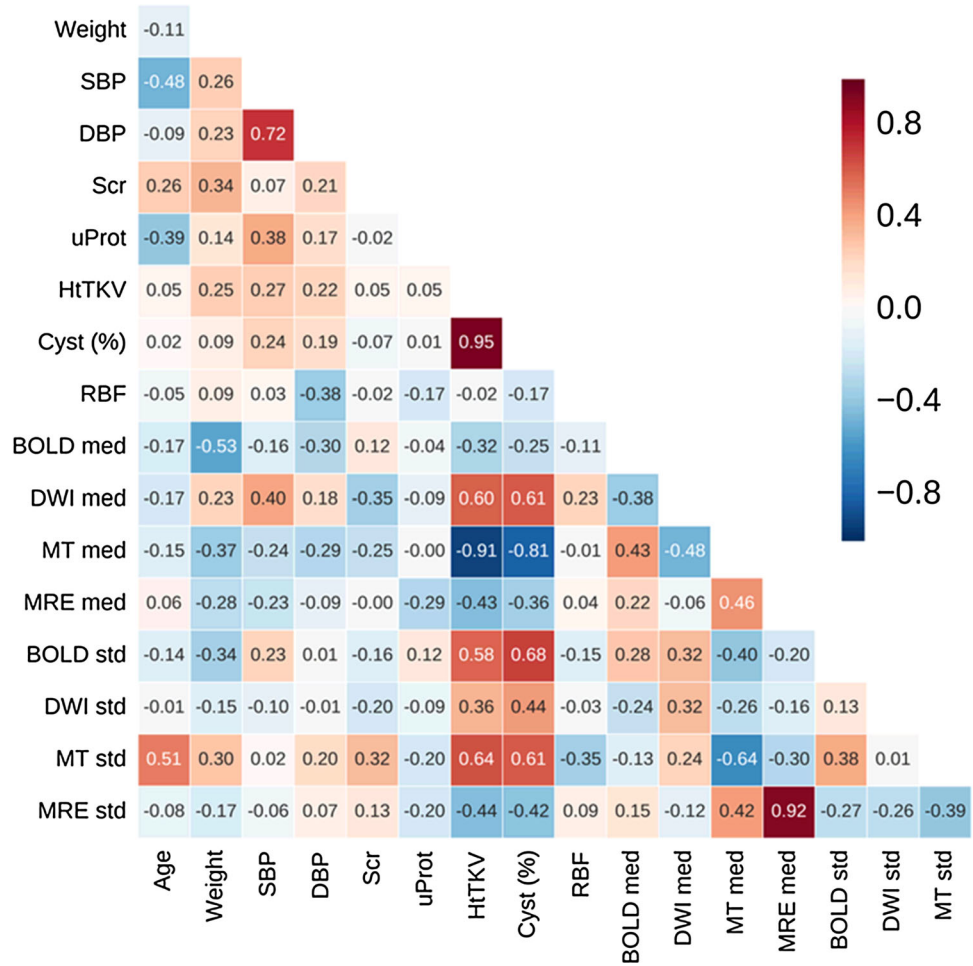
Fig. 3. Bland–Altman analysis of the test–retest reproducibility of the quantitative MR imaging techniques. Ten control controls were imaged on two separate occasions to assess reproducibility. Shown here the results for TKV, RBF,

as well as ADC-derived from DWI, MTR (%) derived from MT, R2\* derived from BOLD, and tissue stiffness derived from MRE. Solid lines show average difference, and dashed lines are confidence intervals (1.96 × SD).

parenchyma in ADPKD patients compared with the controls likely related to decrease turgidity of the kidney with the known phenomenon of decrease in renal blood flow in ADPKD patients [15]. We also found that, compared with cortical measurements, medullary measurements were higher for R2\*, lower for ADC, higher for PF, lower for D, lower for D\*, lower for MTR, and higher for tissue stiffness (data not shown). How these parameters change with disease progression, disease severity, and capability to further refine disease prognosis needs further study.

No strong relationships were found for the derived quantitative parameters with basic characteristics such as age and weight. However, the young cohort used in this study (18–30 years of age) should not be used to rule out any relationships that may exist in a population with larger age variability. Studies with older patients and perhaps a higher number of patients are certainly warranted to address these potential relationships. For instance, very little fibrosis likely exists in these young patients, making aspects of MT and MRE (which can both provide information related to fibrosis) difficult to assess.

Fig. 4. Correlation matrix comparing the main biomarkers considered in this study. Shown here are the relationships for the entire cohort. For the quantitative techniques, both the median (med) and standard deviation (SD) for NCRP are presented.



There are several limitations of the current study. For one, the reproducibility of the quantitative parameters in symptomatic ADPKD patients or those with renal failure was not assessed in the current study. This is a pilot study and we recruited only age- and sex-matched healthy controls and asymptomatic young ADPKD patients. The objective of the study was to determine if quantitative MRI would be useful to detect early changes in the parenchyma. Also, knowledge of how the quantitative parameters progress with the disease, as well as inform on subsequent disease progression is not attainable by the current study. In particular, the sensitivity of these techniques to detect changes over short periods of time will be critical for identifying their utility in clinical trials. There are also a number of functional MRI techniques that were not explored in the current study but may also help characterize the ADPKD kidney. For one, arterial

spin labeling (ASL) offers the opportunity to characterize renal perfusion and could inform on changes in vascular geometry and restrictions in regional kidney blood flow. Lastly, refinement of the current study protocol should be performed to identify the most informative imaging acquisitions in order to reduce imaging and analysis time.

Overall, little research has gone beyond total kidney and cystic volume measurements in the study of ADPKD. For instance, other structural features such as vasculature characterization and measurement of fibrosis are important areas of research which may provide a much clearer picture of the underlying structural changes occurring during the progression of ADPKD. These are details that quantitative MRI techniques can help us address. Therefore, a comprehensive characterization of the ADPKD kidney may be facilitated by MRI to



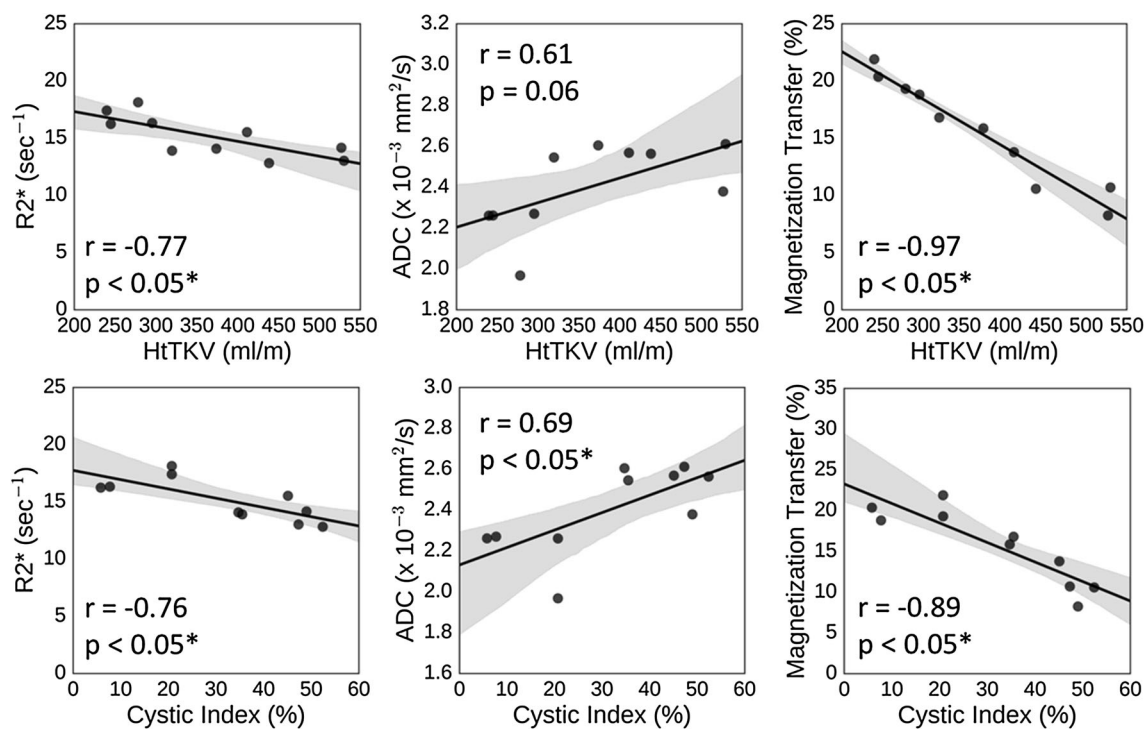


**Fig. 5.** Linear regression analysis for the median whole kidney value measurement for BOLD, DWI, and MT imaging techniques compared with both HtTKV (*top row*), and cystic index (*bottom row*). The *first column* is R2\* derived from BOLD,

the *second* is the ADC value derived from DWI, and the *third* is the MTR value derived from MT. Pearson's *r* is shown, as well as the *p* value. Gray shading is 95% confidence intervals and black solid line is the calculated regression line.

**Table 3.** Characteristics of the 20 patients in this study comparing the controls to the ADPKD patients for quantitative MR measurements

Scan	Parameter	Control	ADPKD	<i>p</i> value
BOLD	R2* (s <sup>-1</sup> )	18.1 ± 1.6	14.9 ± 1.7	0.002*
DWI	ADC (×10 <sup>-3</sup> mm <sup>2</sup> /s)	2.18 ± 0.10	2.46 ± 0.20	0.013*
DWI	PF (%)	15.05 ± 3.97	12.48 ± 3.39	0.121
DWI	D (×10 <sup>-3</sup> mm <sup>2</sup> /s)	2.08 ± 0.21	3.04 ± 1.86	0.005*
DWI	D* (×10 <sup>-3</sup> mm <sup>2</sup> /s)	32.44 ± 17.25	27.65 ± 12.20	0.734
MT	MTR (%)	23.8 ± 1.2	16.3 ± 4.4	<0.001*
MRE	Tissue Stiffness (kPa)	3.8 ± 0.5	3.2 ± 0.3	0.016*

Median for NCRP measurements is shown as mean ± SD. Wilcoxon rank-sum test was used to test for statistical significance (*p* value). A *p* value less than 0.05 was considered significant (denoted with asterisk). R2\* is the BOLD parameter used as a surrogate for the amount of deoxyhemoglobin in the blood. ADC, PF, D, and D\* are measured by DWI. MTR is measured by MT imaging, and Tissue Stiffness is a measure of renal tissue stiffness measured by MRE

NCRP non-cystic renal parenchyma, BOLD blood oxygen level dependent, ADC apparent diffusion coefficient, DWI diffusion weighted imaging, PF perfusion fraction, D true diffusion coefficient, D\* pseudo-diffusion coefficient, MTR magnetization transfer ratio, MRE magnetic resonance elastography

characterize both structural and functional components such as TKV, cystic burden, cyst composition, fibrotic burden, vascular changes, and functional changes in perfusion, oxygenation status, and renal blood flow.

## Conclusions

Quantitative MRI techniques are promising markers for renal disease and could provide additional insights into kidney characterization and disease progression in ADPKD patients. Larger studies are needed to further evaluate quantitative MRI techniques for assessment of renal changes

occurring during the progression of ADPKD and evaluate their applicability in personalized clinical decision making.

### Compliance with ethical standards

**Funding** This work was supported by the National Institute of Diabetes and Digestive and Kidney Diseases under NIH Grant/Award Number P30 DK090728 “Mayo Translational PKD Center (MTPC),” Robert M. and Billie Kelley Pirnie, the PKD Foundation Grant 206g16a, and the National Cancer Institute (NCI) under Grant/Award CA160045.

**Conflict of interest** T.L.K. declares that he has no conflict of interest. M.E.E declares that she has no conflict of interest. I.G. declares that he has no conflict of interest. M.V.I. declares that she has no conflict of

interest. P.K. declares that he has no conflict of interest. P.C.H. declares that he has no conflict of interest. B.F.K. declares that he has no conflict of interest. V.E.T. declares that he has no conflict of interest. S.K.V. declares that he has no conflict of interest. B.J.E. declares that he has no conflict of interest.

**Ethical approval** All procedures performed in studies involving human participants were in accordance with the ethical standards of the institutional and/or national research committee and with the 1964 Helsinki declaration and its later amendments or comparable ethical standards.

**Informed consent** Informed consent was obtained from all individual participants included in the study.

## References

- National Center for Health Statistics, Summary Health Statistics Tables for U.S. Adults: National Health Interview Survey, 2014, Table A-4b, A-4c.
- National Center for Health Statistics, Deaths: Final Data for 2014, Tables 9, 10, 11.
- Smith HW (1953) Compar physiology of the kidney. *J Am Med Assoc* 153:1512–1514
- Myers GL, Miller WG, Coresh J, et al. (2006) Recommendations for improving serum creatinine measurement: a report from the laboratory working group of the National Kidney Disease Education Program. *Clin Chem* 52:5–18
- Coresh J, Astor BC, McQuillan G, et al. (2002) Calibration and random variation of the serum creatinine assay as critical elements of using equations to estimate glomerular filtration rate. *Am J Kidney Dis* 39:920–929
- Zhang JL, Morrell G, Rusinek H, et al. (2014) New magnetic resonance imaging methods in nephrology. *Kidney Int* 85:768–778
- Kajander S, Kallio T, Alanen A, Komu M, Forsstrom J (2000) Imaging end-stage kidney disease in adults. Low-field MR imaging with magnetization transfer vs. ultrasonography. *Acta Radiol* 41:357–360
- Ebrahimi B, Macura SI, Knudsen BE, Grande JP, Lerman LO (2013) Fibrosis detection in renal artery stenosis mouse model using magnetization transfer MRI. *Proc. SPIE* 8672, *Medical Imaging 2013: Biomedical Applications in Molecular, Structural, and Functional Imaging*, 867205 8672:867
- Kline TL, Irazabal MV, Ebrahimi B, et al. (2016) Utilizing magnetization transfer imaging to investigate tissue remodeling in a murine model of autosomal dominant polycystic kidney disease. *Magn Reson Med* 75:1466–1473
- Sourbron SP, Michaely HJ, Reiser MF, Schoenberg SO (2008) MRI-measurement of perfusion and glomerular filtration in the human kidney with a separable compartment model. *Investig Radiol* 43:40–48
- Li LP, Halter S, Prasad PV (2008) Blood oxygen level-dependent MR imaging of the kidneys. *Magn Reson Imaging Clin N Am* 16:613–625
- Pedersen M, Dissing TH, Morkenborg J, et al. (2005) Validation of quantitative BOLD MRI measurements in kidney: application to unilateral ureteral obstruction. *Kidney Int* 67:2305–2312
- Prasad PV, Edelman RR, Epstein FH (1996) Noninvasive evaluation of intrarenal oxygenation with BOLD MRI. *Circulation* 94:3271–3275
- Khatir DS, Pedersen M, Jespersen B, Buus NH (2014) Reproducibility of MRI renal artery blood flow and BOLD measurements in patients with chronic kidney disease and healthy controls. *J Magn Reson Imaging* 40:1091–1098
- King BF, Torres VE, Brummer ME, et al. (2003) Magnetic resonance measurements of renal blood flow as a marker of disease severity in autosomal-dominant polycystic kidney disease. *Kidney Int* 64:2214–2221
- Torres VE, King BF, Chapman AB, et al. (2007) Magnetic resonance measurements of renal blood flow and disease progression in autosomal dominant polycystic kidney disease. *Clin J Am Soc Nephrol* 2:112–120
- Karger N, Biederer J, Lusse S, et al. (2000) Quantitation of renal perfusion using arterial spin labeling with FAIR-UFLARE. *Magn Reson Imaging* 18:641–647
- Martirosian P, Boss A, Schraml C, et al. (2010) Magnetic resonance perfusion imaging without contrast media. *Eur J Nucl Med Mol I* 37:S52–S64
- Warner L, Yin M, Glaser KJ, et al. (2011) Noninvasive In vivo assessment of renal tissue elasticity during graded renal ischemia using MR elastography. *Investig Radiol* 46:509–514
- Maril N, Margalit R, Mispelter J, Degani H (2004) Functional sodium magnetic resonance imaging of the intact rat kidney. *Kidney Int* 65:927–935
- Thoeny HC, De Keyzer F, Oyen RH, Peeters RR (2005) Diffusion-weighted MR imaging of kidneys in healthy volunteers and patients with parenchymal diseases: initial experience. *Radiology* 235:911–917
- Chandarana H, Lee VS, Hecht E, Taouli B, Sigmund EE (2011) Comparison of biexponential and monoexponential model of diffusion weighted imaging in evaluation of renal lesions: preliminary experience. *Investig Radiol* 46:285–291
- Wang F, Kopylov D, Zu Z, et al. (2015) Mapping murine diabetic kidney disease using chemical exchange saturation transfer MRI. *Magn Reson Med* 76(5):1531–1541
- Kline TL, Edwards ME, Korfiatis P, et al. (2016) Semiautomated segmentation of polycystic kidneys in T2-weighted MR images. *Am J Roentgenol* 207:605–613
- Altman DG, Bland JM (1983) Measurement in medicine—the analysis of method comparison studies. *Statistician* 32:307–317
- Bland JM, Altman DG (1986) Statistical methods for assessing agreement between two methods of clinical measurement. *Lancet* 1:307–310
- Sesso HD, Stampfer MJ, Rosner B, et al. (2000) Systolic and diastolic blood pressure, pulse pressure, and mean arterial pressure as predictors of cardiovascular disease risk in men. *Hypertension* 36:801–807
- Spiering W, Kroon AA, Fuss-Lejeune MM, Daemen MJ, de Leeuw PW (2000) Angiotensin II sensitivity is associated with the angiotensin II type 1 receptor A(1166)C polymorphism in essential hypertensives on a high sodium diet. *Hypertension* 36:411–416